

Article

Experimental and Numerical Study of Strengthening Prestressed Reinforced Concrete Beams Using Different Techniques

Ahmed S. Eisa¹ , Kamila Kotrasova^{2,*} , Peter Sabol³, Mária Mihaliková⁴  and Mohamed G. Attia^{1,*} ¹ Structural Engineering Department, Zagazig University, Zagazig 44519, Egypt; ahmedeisa@zu.edu.eg² Institute of Structural Engineering and Transportation Structures, Faculty of Civil Engineering, Technical University of Kosice, Vysokoskolska 4, 04200 Kosice, Slovakia³ Laboratory Center CVIS, The Faculty of Civil Engineering, Technical University in Kosice, 04200 Kosice, Slovakia; peter.sabol@tuke.sk⁴ Institute of Materials and Quality Engineering, Faculty of Materials, Metallurgy and Recycling, Technical University of Kosice, Letna 1/9, 04200 Kosice, Slovakia; maria.mihalikova@tuke.sk

* Correspondence: kamila.kotrasova@tuke.sk (K.K.); mohgoudaattia@gmail.com (M.G.A.)

Abstract: This study aimed to evaluate the static response of prestressed reinforced concrete beams strengthened in their flexure and shear properties using different strengthening techniques, steel plates, and externally bonded woven carbon fiber fabric (WCFF). The experimental work involved testing twenty large-scale prestressed reinforced concrete beams with a length of 3000 mm, and cross-sections measuring 400 mm in height and 200 mm in breadth were cast in the factory and tested in the laboratory. Four beams without prestressing served as the reference beams; two unbonded prestressed beams served as the control beams, and the remaining fourteen beams were strengthened with steel plates and externally bonded woven carbon fiber fabric (WCFF). Eight of the beams were strengthened with 4 mm thick steel plates and tested under a monotonically increasing load with manual readings recorded. The remaining six beams were strengthened with 0.5 mm thick WCFF and tested under a monotonically increasing load with manual readings recorded. The variables considered included the strengthening techniques (FRP composite sheets, steel plates), the types of strengthening (slices, U-shaped), and the flexural and shear capacities of the strengthened beams. All the implemented strengthening techniques yielded enhancements in both the flexural and shear strength outcomes of the beams compared to their respective controls. The most significant increase in load capacity, whether in terms of ultimate load or first crack load, for the prestressed concrete beams' flexure properties occurred when strengthening with U-shaped steel plates. Additionally, the greatest reduction in deflection at the point of reaching the maximum load for the prestressed concrete beams, in terms of their flexure properties, was observed when strengthening with U-shaped steel plates. Similarly, the maximum load increase for the prestressed concrete beams, in terms of their shear properties, was achieved through strengthening with U-shaped woven carbon fiber fabric wrapping. Furthermore, a finite element model was created to simulate various experimental specimens. The finite element model's results exhibited harmony with the experimental results, affirming the efficacy of the presented finite element model.

Keywords: prestressed; pre-tension; beams; WCFF; steel plates; flexure; shear

Citation: Eisa, A.S.; Kotrasova, K.; Sabol, P.; Mihaliková, M.; Attia, M.G. Experimental and Numerical Study of Strengthening Prestressed Reinforced Concrete Beams Using Different Techniques. *Buildings* **2024**, *14*, 29. <https://doi.org/10.3390/buildings14010029>

Academic Editor: Chuang Feng

Received: 20 November 2023

Revised: 13 December 2023

Accepted: 18 December 2023

Published: 21 December 2023



Copyright: © 2023 by the authors. Licensee MDPI, Basel, Switzerland. This article is an open access article distributed under the terms and conditions of the Creative Commons Attribution (CC BY) license (<https://creativecommons.org/licenses/by/4.0/>).

1. Introduction

Structure plays an important role in the development of individuals, states, or countries. A structure consists of three main elements, namely, the beam, the column, and the slab. All three of these elements have their importance. Beams are one of the most important structural elements of any structure; they can be part of a bridge, industrial building, road, etc. Beams must be designed to carry all types of loads without causing deformation or cracking of the structure. But, sometimes, beams can be subjected to sudden static loads that they are not designed to withstand. Because of these sudden loads, beams tend to

crack [1,2]. This is mainly due to the tension or compression of the beam. Prestressed concrete beams are used in buildings that need to support heavy loads, such as bridges, industrial buildings, etc. [3]. These beams have smaller beam depths and better shear strength. These beams are most commonly used where the span is greatest. Reinforcement should be applied to protect a beam from cracking due to fatigue loading, reducing the number and dimensions of cracks. In practice, traditional techniques such as joining steel plates, concrete encasing, and external restraints are common. Steel plate jacketing of beams has been successfully used for seismic retrofitting of structures where corrosion is not a critical issue. Reinforcement using steel plates is a widely adopted method due to its advantages, including rapid construction, cost-effectiveness, and a notable strengthening impact, especially for prestressed beams [4]. Typically, steel plates are affixed to the girder using structural adhesives or epoxy resin and secured to either the tensile edge or the vulnerable surface of the beam. This integration forms a cohesive force with the beam, essentially functioning as additional steel bars, thereby enhancing the overall strength [5]. In comparison to reinforcing with bonded fibers, employing steel plates fully exploits the mechanical properties inherent to steel plates [6]. Steel plates are readily available and relatively economical [7], possessing characteristics such as uniform stress distribution and favorable plasticity [8]. Strengthening with steel plates has demonstrated its effectiveness in improving stiffness, minimizing deformation under live loads [9], fortifying crack resistance [10], and, notably, enhancing the bending [11] and shear performance of the primary girder [12]. Importantly, this method has no significant impact on a structure's appearance or headroom [13]. However, fiber-reinforced polymers (FRP) have emerged as highly promising materials for both rehabilitating existing reinforced concrete structures and fortifying new civil engineering constructions [14]. Contemporary composite materials, utilizing non-metallic continuous fibers, are progressively employed in civil engineering applications for the purpose of enhancing the structural integrity of buildings [15]. This preference is attributed to their numerous benefits, including a high strength-to-weight ratio, robust fatigue resistance, flexibility, ease of handling, and outstanding durability. The failure mode in terms of the shear properties of a reinforced concrete (RC) beam differs significantly from flexural failure, with the latter being ductile and the former exhibiting a brittle and catastrophic nature. In instances where an RC beam lacks sufficient shear strength or when its shear capacity is lower than the flexural capacity post-strengthening, addressing shear strengthening becomes imperative. Evaluating the shear capacity of RC beams intended for flexural strengthening is of utmost importance [16]. Research exploring the efficacy of externally bonding fiber-reinforced polymer (FRP) plates onto prestressed concrete beams has yielded evidence showcasing heightened load-carrying capacity and post-cracking stiffness. The failure mode observed during flexural testing involved FRP rupture and de-bonding [16–18]. Further experimental investigation into the static behavior of prestressed concrete beams strengthened with externally bonded glass fiber-reinforced polymer (GFRP) demonstrated superior performance in terms of ultimate load, deformation, and ductility indices compared to the control beam [19]. The findings from these studies strongly advocate for the application of externally bonded FRP, highlighting a substantial increase in strength and control over deflection for both reinforced and prestressed concrete beams [20]. The present study aims to assess the performance characteristics of prestressed concrete beams reinforced with woven carbon fiber fabric (WCFF) and steel plates under monotonic loading conditions.

2. Materials and Methods

2.1. Experimental Plan

The experimental plan included testing sixteen large-scale prestressed R.C. beams in addition to four non-prestressed R.C. beams as reference. The beams were 400 mm in height, 200 mm in cross-section breadth, and 3000 mm in length. The beam specimens were divided into four models. The first model was used for flexural testing. The first model of beam specimen utilized two 12 mm diameter bars for tension reinforcement in

the longitudinal steel. Additionally, two high-tensile 12.5 mm diameter prestressing wires with 50 mm eccentricity were incorporated, along with two 10 mm diameter bars as the hanger bars. Two-legged 10 mm diameter stirrups were spaced at 150 mm intervals. For shear testing of the second model, the longitudinal steel comprised two 18 mm diameter bars for tension reinforcement. The prestressing system included two high-tensile 12.5 mm diameter wires with 50 mm eccentricity. As for the hanger bars, four 22 mm diameter bars were employed, and two-legged 8 mm diameter stirrups were provided at 300 mm intervals along the beam. Detailed reinforcement configurations are visually presented in Figures 1 and 2.

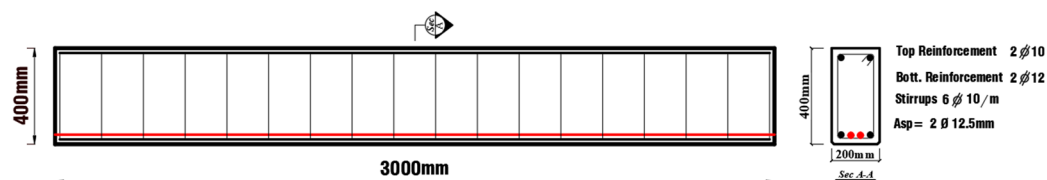


Figure 1. Reinforcement details of the first model for flexure testing.

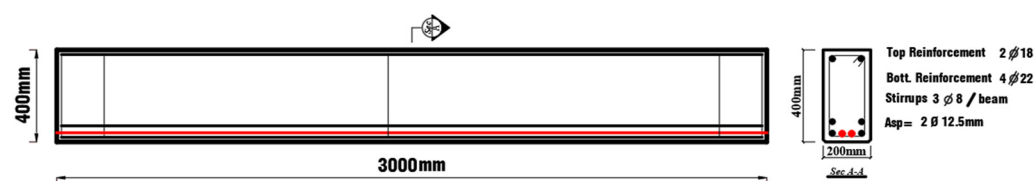


Figure 2. Reinforcement details of the second model for shear testing.

Two prestressed concrete beams without strengthening were considered to be the control beams; seven beams were strengthened with steel plates, and seven beams were strengthened with woven carbon fiber fabric (WCFF). Under two-point loading conditions, all the beams underwent testing, and their performance characteristics were evaluated in the presence of monotonic loading. The experimental outcomes, including load, deflection, and crack data, were recorded. For a comprehensive overview of the beams, refer to Table 1.

Table 1. Sample description.

Sample	Strengthening Type	Connection Type
Flexural strengthening		
CF	No strengthening (Control beam)	-
FB1, FB2	Bottom steel plate (U-shape)	Anchors
FB3, FB4	Bottom steel plate	Anchors
FB5, FB6	Bottom WCFF (U-Shape)	Adhesive
FB7	Bottom WCFF	Adhesive
Shear strengthening		
CS	No strengthening (Control beam)	-
SB1, SB2	Steel plate (U-shape)	Anchors
SB3, SB4	Steel plate (Straps)	Anchors
SB5, SB6	WCFF (U-Shape)	Adhesive
SB7	WCFF (Straps)	Adhesive

2.2. Material Characteristics

Concrete with a compressive strength of 40 MPa was used when uniaxial compressive tests on the specimens (150 mm × 150 mm × 150 mm concrete cube) were performed, and

the average concrete compressive strengths at 7 and 28 days are shown in Table 2. Steel bars of different diameters (10, 12, 18, and 22 mm) were used for the main reinforcement, having 440 MPa tensile strength, and steel bars of varying diameters (8 and 10 mm) were used for the stirrups. Steel plates with a thickness of 4 mm and 345 MPa tensile strength were used as external reinforcements. Table 3 provides the detailed properties of both the steel bars and the plates. Prestressing wires with a tensile strength of 1860 MPa were used, and the detailed properties of the strands are presented in Table 4. Woven carbon fiber fabric, with a tensile strength of 4300 MPa, was applied to the beam specimens' surface using epoxy adhesive. Detailed properties of the Woven Carbon Fiber Fabric are outlined in Table 5.

Table 2. Compressive strength test results.

Specimen ID	Average Cube Compressive Strength after 7 Days (MPa)	Average Cube Compressive Strength after 28 Days (MPa)
SB1	25.9	38.6
SB2	25.6	35.6
SB3	27.8	40.8

Table 3. Properties of steel reinforcement.

Reinf.	Bar Dia. (mm)	Plate Thick. (mm)	Yield Stress (MPa)	Ult. Stress (MPa)	Modulus of Elasticity (MPa)
Steel Bars	8	-	470	575	210,000
	10	-	450	550	211,000
	12	-	440	530	207,000
	18	-	490	581	200,000
	22	-	492	595	205,000
Steel Plate	-	4	345	420	206,000

Table 4. Properties of prestressing strands.

Diameter (mm)	Tensile Strength (MPa)	Mass (g/m)	Cross-Sectional Area (mm ²)	Minimum Breaking Strength (kN)	Maximum Breaking Strength (kN)
12.5	1860	726.3	93.0	173.0	199.0

Table 5. Properties of WCFF.

Thickness (mm)	Fiber Density (g/cm ³)	Tensile Strength (MPa)	Ultimate Elongation (%)	Elasticity Modulus (MPa)
0.131	1.76	4300	1.8	238,000

3. Preparation of Test Beams

Plywood was prepared for the beam samples. Steel reinforcement cages were prepared for each specimen. The high-tensile steel wire was placed 150 mm below the centerline of the cross-section. Each beam was provided with two high-tensile steel wires. The high-tensile steel wires were stretched before the beam specimens were cast. The interior portion of the plywood was applied with a coating of oil to prevent concrete from adhering to the

plywood. The required quantity of concrete was mixed in a motorized mixture machine. The concrete was placed in layers up to the top of the beam specimens, and adequate compaction was carried out using a needle vibrator to avoid honeycombing. The beam specimens were demolded after 7 days of casting, and the high-tensile steel wires were cut. The beam specimens were cured by painting Sika® Antisol® WB, Sika Egypt, El Obour City, Egypt.

3.1. Strengthening by WCFF

To create a textured surface, coarse sandpaper was employed, and the designated concrete region was thoroughly cleaned using an air blower to eliminate any dirt or debris particles. Following the surface preparation process, epoxy resin was meticulously mixed as per the manufacturer's instructions. The fabrics were cut to size, ensuring uniform blending, and the epoxy resin was applied to the concrete surface. Subsequently, the woven carbon fiber fabric (WCFF) layer was positioned atop the epoxy resin coating. Six beam specimens were utilized for both flexural and shear tests. Among them, three beam specimens underwent strengthening with WCFF for the flexural tests, while the remaining specimens were reinforced with WCFF for the shear tests. The details of the strengthening process are shown in Figures 3–6.

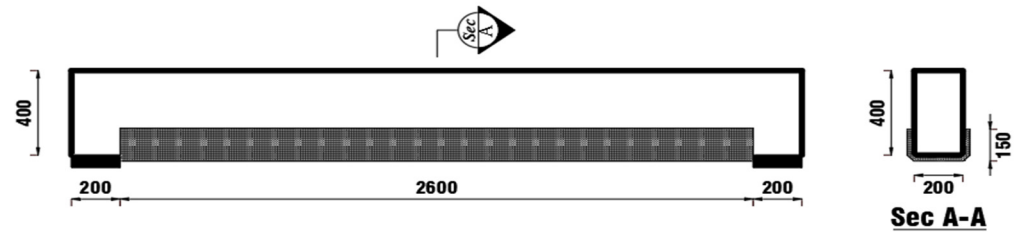


Figure 3. (FB5, FB6) Flexural strengthening using WCFF [U-shaped].

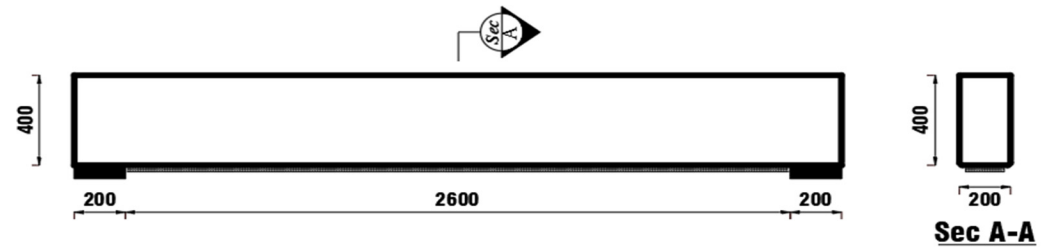


Figure 4. (FB7) Flexural strengthening using WCFF slice.

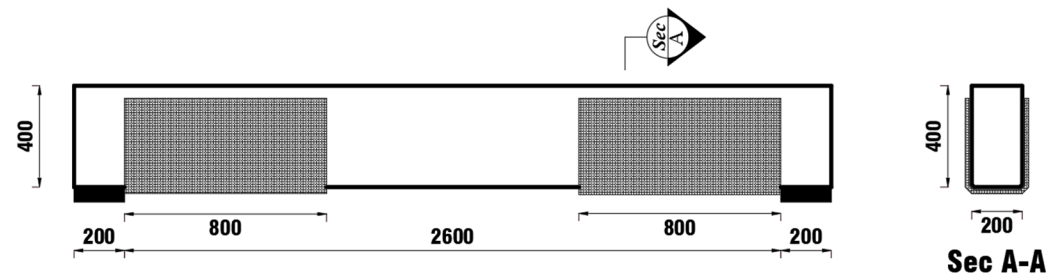


Figure 5. (SB5, SB6) Shear strengthening using WCFF.

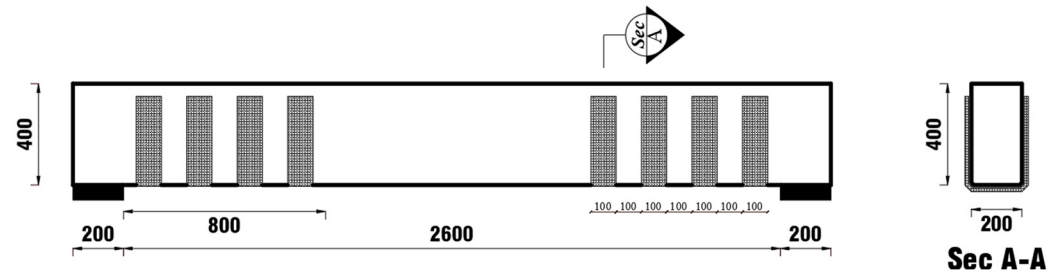


Figure 6. (SB7) Shear strengthening using WCFF straps.

3.2. Strengthening by Steel Plates

The concrete surface was cleaned. The steel plates were cut, fixed on the surface of the concrete beams in the places specified for them, and then punched with a drill. Bolts were placed in their indicated locations and fixed with a spanner. Eight beam specimens were used for the flexural and shear tests. Four beam specimens were strengthened with steel plate for the flexural tests, and the rest of the beam specimens were strengthened with steel plate straps for the shear tests. The details of the strengthening process are shown in Figures 7–10.

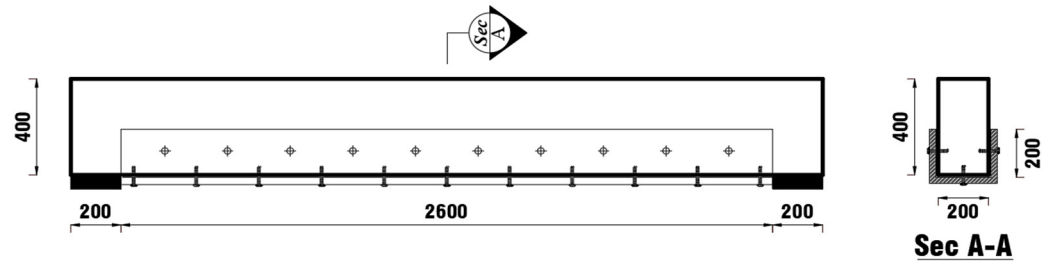


Figure 7. (FB1, FB2) Flexural strengthening using a steel plate [U-shaped].

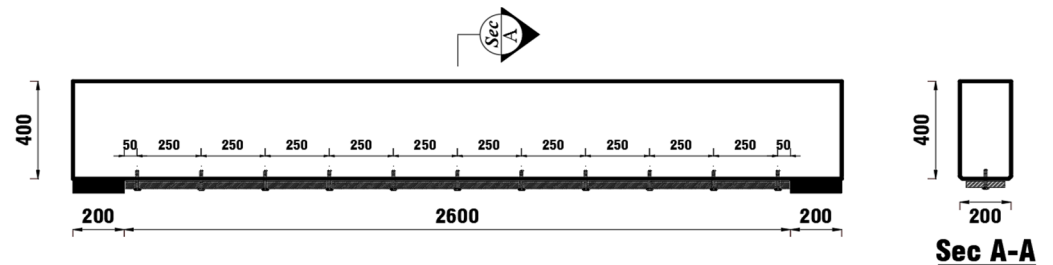


Figure 8. (FB3) Flexural strengthening using a steel plate slice.

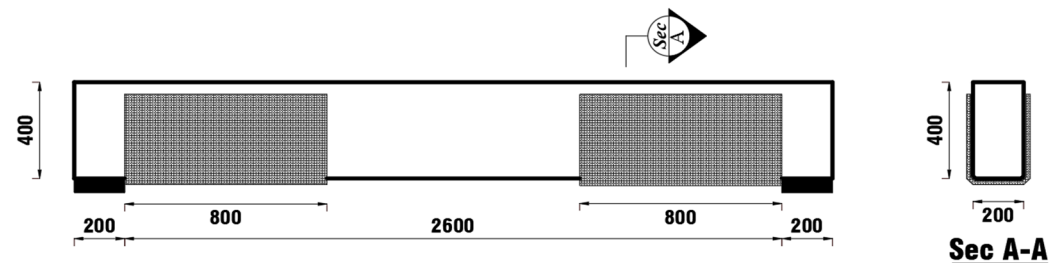


Figure 9. (SB1, SB2) Shear strengthening using a steel plate [U-shaped].

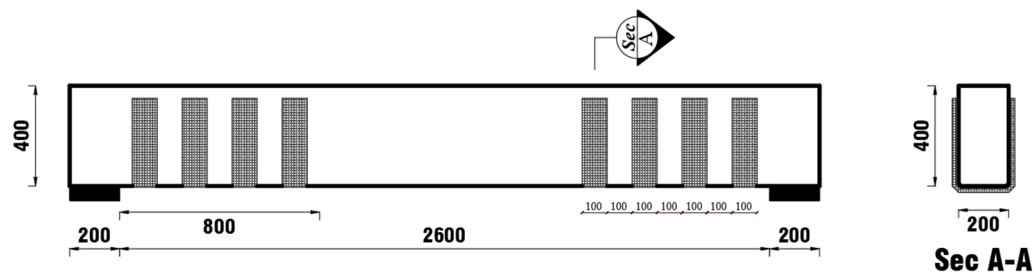


Figure 10. (SB3) Shear strengthening using steel straps [U-shaped].

4. Testing Procedure

To evaluate the performance, the prestressed beams reinforced with both steel plates and woven carbon fiber fabric (WCFF) underwent testing using a two-point loading system within a 100 ton capacity loading frame. The beam was supported with one end hinged and the other end equipped with a roller. The application of the load was accomplished using a hydraulic jack, and load measurements were obtained from the load cell. Refer to Figure 11 for a visual representation of the beam test setup.



Figure 11. Loading test setup.

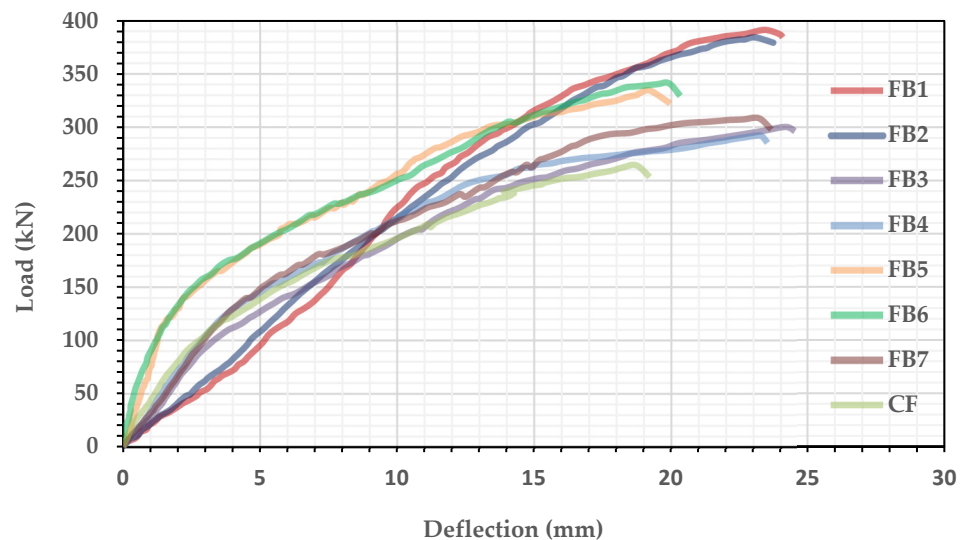
5. Results and Discussion

5.1. Flexural Test Series

All test results for both the strengthened and non-strengthened beams, in terms of their flexure properties, are detailed in Table 6, while the load versus deflection graph is illustrated in Figure 12. The load–deflection curve reveals three distinct behavioral regions. Initially, the concrete displayed linear–elastic behavior, exhibiting high beam stiffness. As loading increased, the stresses in the outermost woven carbon fiber fabric (WCFF) and steel plates elevated the tensile strength of the concrete, resulting in the formation of flexural cracks in the constant moment area. This led to a decrease in beam stiffness due to flexural cracking. Notably, the results indicate that strengthening with steel plates outperformed strengthening with WCFF, enhancing the bearing strength of the prestressed beam by 20% compared to the WCFF reinforcement. Regarding the max mid-span deflection, the beams strengthened with steel plates experienced a slight increase, not exceeding 4%, compared to those reinforced with carbon fiber. Comparing the load–deflection relationships for the prestressed concrete beams, it becomes evident that strengthening the beams with U-shaped layers at the bottom significantly improved their load-carrying capacity.

Table 6. Strength and deformation at various load stages for the flexural test series.

No.	Specimen	F.C.L (kN)	Deflection of F.C.L (mm)	Maximum Load (kN)	Deflection of Maximum Load (mm)	Strengthening Type	Connection Type
1	CF	58	1.40	264	18.74	(Control beam)	-
2	FB1	110	2.84	391	23.46	Bottom steel plate (U-shape)	Anchors
3	FB2	114	2.90	384	23.06		
4	FB3	91	1.99	300	24.18	Bottom steel plate	Anchors
5	FB4	92	2.02	292	23.24		
6	FB5	77	0.90	334	19.25	Bottom WCFF (U-Shape)	Adhesive
7	FB6	78	0.92	341	19.92		
8	FB7	74	1.3	308.2	23.2	Bottom WCFF	Adhesive

**Figure 12.** Relationship between load and deflection for the flexural test series.

5.1.1. Effect of Strengthening at Various Loads

Figure 12 illustrates the impact of woven carbon fiber fabric (WCFF) and steel plates on various load levels of prestressed concrete beams. Specifically, prestressed concrete beams strengthened with 0.5 mm thick U-shaped WCFF and WCFF slices demonstrated increases of 29% and 17%, respectively, at the ultimate load stage compared to the control beam. In the case of beams strengthened with 4 mm thick U-shaped steel plates and steel plate slices, there were increases of 48% and 14%, respectively, at the ultimate load stage compared to the control beam. Notably, beam FB1 exhibited the highest load-carrying capacity, approximately 1.48 times that of the control beam. The results indicate that prestressed concrete beams strengthened with U-shaped layers show enhanced load-carrying capacity ranging from 10% to 30% compared to prestressed concrete beams strengthened with slice layers, whether strengthened using steel plates or WCFF. This highlights the effectiveness of U-shaped layers in improving the structural performance of prestressed concrete beams.

5.1.2. Effect of Strengthening on Deflections

The deflection of a prestressed concrete beam is primarily influenced by factors such as load, length, moment of inertia, and the elastic modulus of concrete. Strengthening with woven carbon fiber fabric (WCFF) and steel plates contributes to an increase in the cross-section and rigidity of the prestressed concrete beam. This heightened stiffness impacts the bending behavior of the wrapped beams across various stages, including pre-

failure, failure, and post-failure. In particular, at the ultimate load stage, the deflection of strengthened prestressed concrete beams increased by 25% for 4 mm steel plates (U-shaped) and 29% for bottom steel plates. Conversely, the deflection for the prestressed concrete beams strengthened with 0.5 mm woven carbon fiber fabric (U-shaped) and the bottom woven carbon fiber fabric decreased by 38% and 27%, respectively, compared to the control beam. These findings underscore the role of strengthening materials and configurations in influencing the deflection characteristics of prestressed concrete beams, with variations observed based on the type and placement of the reinforcements.

5.2. Shear Test Series

All the tested prestressed beams exhibited a brittle shear failure mode, characterized by the development of diagonal tension cracks in the constant shear span. In beams externally strengthened with woven carbon fiber fabric (WCFF), diagonal cracking was followed by WCFF debonding, with failure occurring at a significantly higher load than that for the non-strengthened prestressed beams. In contrast, the beams externally strengthened with steel plates displayed only diagonal cracking in all the prestressed beams, with no distortions occurring in the steel plates. The results indicate that strengthening with woven carbon fiber fabric is more effective than strengthening with steel plates, as it increased the shear strength capacity of the prestressed beam by 12% compared to strengthening with steel plates. Regarding the max mid-span deflection, the deflection of prestressed beams strengthened with woven carbon fiber fabric decreased by 20% compared to the beams strengthened with steel plates. Detailed results for both the strengthened and non-strengthened shear beams are presented in Table 7, and the load versus deflection graph is depicted in Figure 13.

Table 7. Strength and deformation at various load stages for the shear test series.

No.	Specimen	F.C.L (kN)	Deflection of F.C.L (mm)	Maximum Load (kN)	Deflection of Maximum Load (mm)	Strengthening Type	Connection Type
1	CS	112	1.74	258	2.9	(Control beam)	-
2	SB1	182	2.65	412	14.94	Steel plate (U-Shape)	Anchors
3	SB2	175	2.32	407	15.46		
4	SB3	120	2.73	291	9.88	Steel plate (Straps)	Anchors
5	SB4	114	2.44	286	9.46		
6	SB5	148	2.26	462	12.46	WCFF (U-Shape)	Adhesive
7	SB6	144	2.29	456	12.84		
8	SB7	133	1.79	374	15.44	WCFF (Straps)	Adhesive

5.2.1. Effect of Strengthening at Various Loads

Figure 13 shows the effect of WCFF laminates and steel plates on various load levels of prestressed concrete beams. The 0.5 mm thick WCFF (U-shaped)- and WCFF straps-strengthened prestressed concrete beams show increases of 77.9% and 44.9%, correspondingly, at the ultimate load stage in comparison with the control beam. In the case of the prestressed concrete beams strengthened with 4 mm thick steel plates (U-shaped) and steel plate straps, the strengthened beams show increases of 58.7% and 11.8%, correspondingly, at the ultimate load stage in comparison with the control beam.

5.2.2. Effect of Strengthening on Deflections

The deflection of the strengthened prestressed concrete beams increased at the ultimate load stage for the 4 mm steel plates (U-shaped) and steel plate straps by 424.14% and 233.44%, respectively. The prestressed concrete beams straightened using 0.5mm WCFF

(U-shaped) and straps of WCFF exhibited increases of 336.2% and 432.4% in the deflection comparison with the control beam.

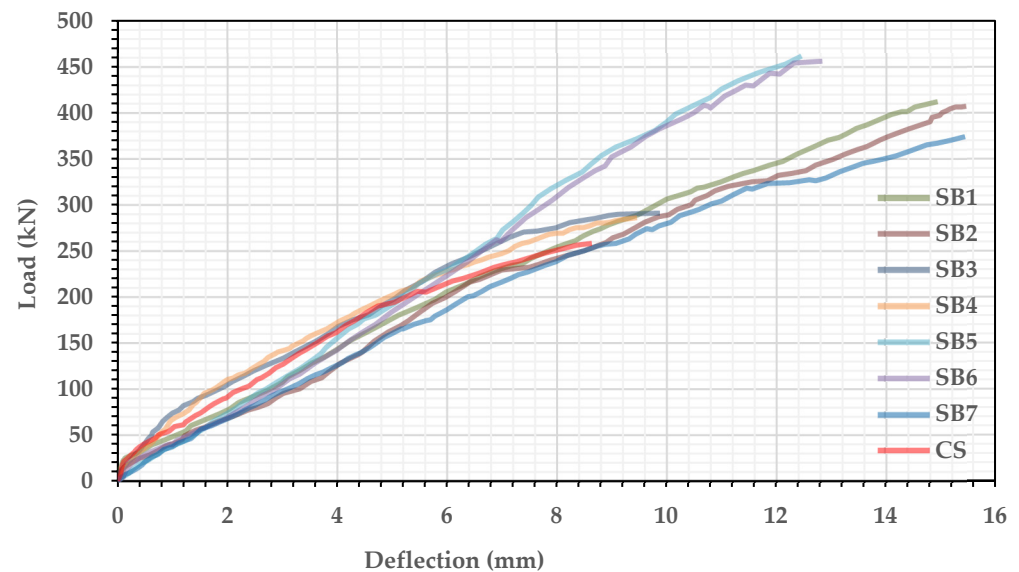


Figure 13. Relationship between load and deflection for the shear test series.

6. Failure Modes and Cracking Patterns

Figures 14 and 15 show the tested beams' failure modes for the flexural and shear test series. An inspection of Figure 14 suggests that all the beams experienced flexural failure, and Figure 15 suggests that all the beams experienced shear failure. For the flexural test series, the presence of the steel plates and WCFF (U-shaped) at the bottom of beams FB1 and FB2 limited the propagation of flexural cracks. The rest of the various strengthening techniques for prestressed concrete beams did not limit the propagation of flexural cracks. Beams FB3, FB4, and FB7 failed in a compressive mode by crushing concrete, while beams FB5 and FB6 failed in a tensile mode by means of a rupture in the WCFF. As for the shear test series, the presence of U-shaped steel plates for the prestressed concrete beams (SB1, SB2) led to a reduction in the propagation of shear cracks, while the different strengthening techniques for prestressed concrete beams did not limit the propagation of shear cracks. Beams SB5, FB6, and FB7 failed in shear compression failure by crushing in the concrete and rupturing in the WCFF, while beams FB3 and FB4 failed in shear compression failure by crushing in the concrete only.



Figure 14. Cracks of the samples in failure mode for the flexural test series.

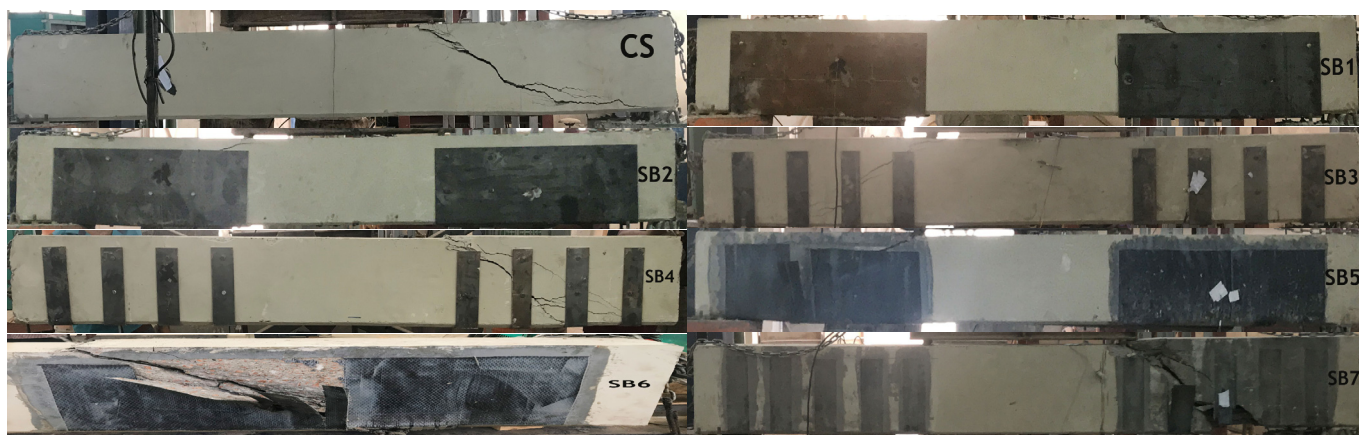


Figure 15. Cracks of the samples in failure mode for the shear test series.

7. Simulation Finite Element Model

Finite element modeling (FEM) has become a widely employed method for studying the structural behavior of various elements. Numerous software packages have been developed to numerically analyze the structural response to flexural and shear stresses using finite element (FE) techniques. In this study, to gain a comprehensive understanding of the behavior of reinforced concrete beams under flexural and shear conditions, an FE model was created to simulate different specimens. Abaqus/CAE was utilized for the analysis in this study. Abaqus/CAE is a versatile analysis product that employs a standard static FE formulation. It is well-suited to modeling various loading conditions, including ramping loading and uniform static pressures. Additionally, it is highly efficient in handling highly nonlinear problems, especially those involving changing contact conditions, such as forming simulations. The FE model analysis was constructed based on the geometric, structural specifications, and material properties of the experimented beam models mentioned earlier. This approach provides a valuable tool for simulating and understanding the complex structural behavior of reinforced concrete beams subjected to flexure and shear stresses [21].

7.1. Finite Element Modeling

To construct the finite element (FE) model, a 3D FE mesh was generated for the concrete beams, wires, strengthening steel plates, reinforcement bars, and woven carbon fiber fabric (WCFF). Three main types of elements were used—solid elements, truss elements (wire elements), and shell elements—via the following steps:

1. Concrete beams were modeled using solid elements, specifically the C3D8R or brick elements.
2. Reinforcement bars and stirrups were modeled using the T3D2 element, which represents truss elements. These elements were embedded in the concrete blocks.
3. WCFF were modeled using conventional shell elements. Two types of shell elements were employed—S8R5 for thin-shell elements and S8R for thick-shell elements.

This combination of solid, truss, and shell elements allows for a detailed and accurate representation of the complex geometry and material interactions in the FE model. The chosen elements are tailored to the specific characteristics of each component, enabling a comprehensive simulation of the structural behavior of the reinforced concrete beams and their strengthening elements.

7.2. Material Modeling

In the modeling of the reinforced concrete (RC) beams, various material models were applied, and, while efforts were made to specify material properties for all the elements, obtaining high-quality material data, especially for more complex models like material damage properties, proved challenging. The accuracy and reliability of the results are

inherently limited by the precision and comprehensiveness of the available material data. For modeling RC beams, the following three material models were used:

1. Concrete material model: The concrete damaged plasticity model available in Abaqus was employed to model concrete.
2. Reinforcement bars: An elastic–plastic model was used to represent the reinforcement bars embedded in the concrete elements.
3. Woven carbon fiber fabric (WCFF): An elastic-lamina model was used to simulate the WCFF.

Tables 8 and 9 detail the concrete elastic properties and parameters for the concrete damaged plasticity model used in the analysis. Two types of steel reinforcement were utilized: high-tensile bars with diameters of 22, 18, 12, and 10 mm to represent the main longitudinal reinforcement bars and steel bars with diameters of 10 mm and 8 mm to represent the stirrups. Table 10 presents the properties of the steel reinforcement used to model the longitudinal bars and the stirrups. The WCFF was modeled as an orthotropic elastic lamina in Abaqus, incorporating characteristics such as Young’s modulus (E_1 , E_2), Poisson’s ratio (ν_{12}), shear modulus (G_{12} , G_{13} , G_{23}), and stress limit (sub-option-fail stress), as outlined in Table 11. These material models and properties contributed to a comprehensive representation of the behavior of the different components in the FE model.

Table 8. Elastic properties of concrete.

Parameter	Model (1)	Model (2)	Model (3)
Mass density, kg/m^3	2400	2400	2400
Modulus of elasticity (E_s), MPa	17,864	22,736.58	23,424.77
Poisson’s ratio (ν)	0.14	0.16	0.17

Table 9. Concrete damaged plasticity parameters.

Parameter	Dilation Angle	Eccentricity	f_b/f_{c0}	K	Viscosity p.
Model (1)	41	0.8	1.16	0.667	0.000001
Model (2)	49	0.04	1.18	0.667	0.000001
Model (3)	37	0.1	1.16	0.667	0.000001

Table 10. Elastic properties of steel reinforcement.

Parameter	High Tensile	Normal–Mild
Mass density, kg/m^3	7859	7859
Modulus of elasticity (E_s), MPa	210,000	203,000
Poisson’s ratio (ν)	0.3	0.3
Yield stress, MPa	490	470
Ultimate stress, MPa	581	575
Elongation, %	15	23

Table 11. Properties of the WCFF material.

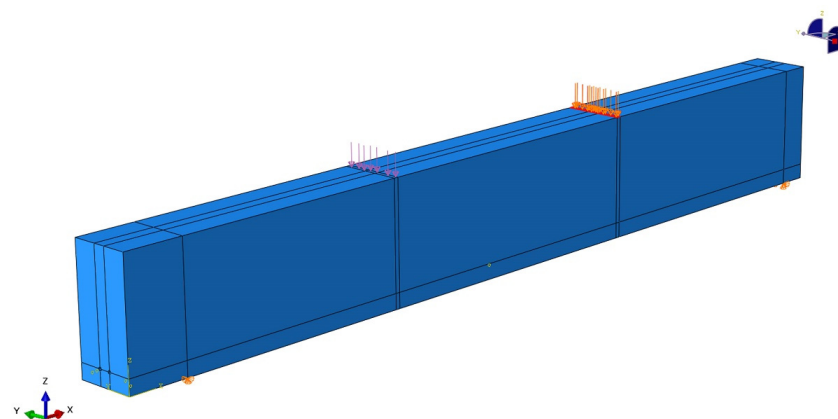
Parameter	WCFF
Mass density, kg/m^3	1760
Modulus of elasticity (E_1), MPa	238,000
Modulus of elasticity (E_2), MPa	238,000
Poisson’s ratio (ν_{12})	0.23

Table 11. *Cont.*

Parameter	WCCF
Shear modulus (G12), MPa	7800
Shear modulus (G13), MPa	7800
Shear modulus (G23), MPa	7800
Stress limit (tensile strength), MPa	4300
Thickness, mm	0.131

7.3. Boundary Conditions

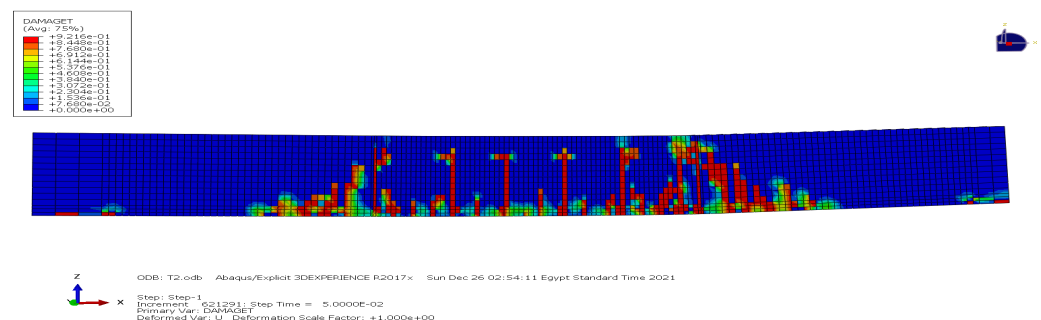
In the Abaqus model tree, boundary conditions can be added using * the load options and choosing * to create a boundary condition. A fixation was made for the two steel parts that represent roller supports in all directions, relying on the interaction between the concrete beam and the roller's surface to reach the closest possible behavior to the experimented samples, as shown in Figure 16.

**Figure 16.** Boundary condition of the model.

7.4. Finite Element Model Results for the Flexural Test Series

7.4.1. Control Beam (CF)

In the flexural damage test, the control beam with cables experienced ultimate failure at a load of 266.44 kN. The initiation of the first crack occurred at a load of 63.27 kN. Figure 17 visually represents the crack pattern observed in the control beam with cables (CF) after testing. This figure provides insights into the nature and extent of cracking within the beam. For a further analysis of the structural response, Figure 18 illustrates the maximum deflection of the control beam. The maximum deflection for the sample reached 32.63 mm, while the average mid-span deflection was 8.62 mm. These measurements help us characterize the deformation and overall performance of the control beam under the applied loading conditions.

**Figure 17.** Damage of FE model for control beam CF.

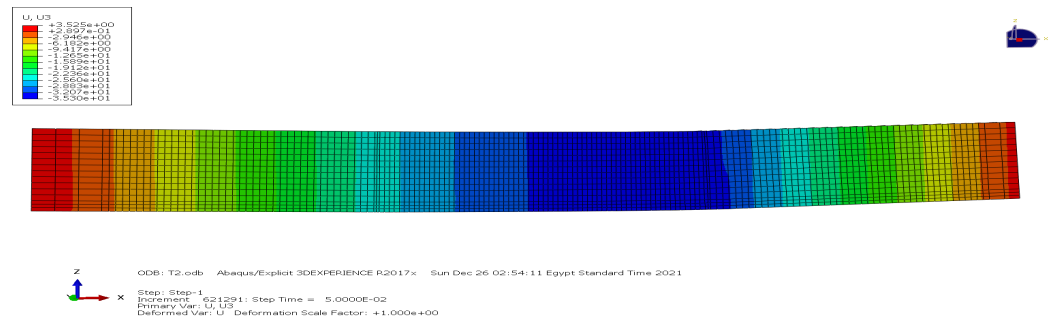


Figure 18. The max deflection of the FE model for control beam CF.

7.4.2. Addition of Steel Plate and WCFF (U-Shaped) to the Tension Side (FB1, FB5)

In the flexural damage tests, the beams equipped with a U-shaped steel plate and woven carbon fiber fabric (WCFF) experienced ultimate loads of 402.55 kN and 335.75 kN, respectively. The initiation of the first crack occurred at loads of 120.76 kN and 83.93 kN for the U-shaped steel plate and WCFF models, respectively. Figure 19 visually depicts the crack patterns observed in FB1 and FB5 after testing. These figures provide insights into the failure modes and crack propagation within the beams. For a more detailed understanding of stress distribution, Figure 20 showcases the stress distribution of the steel plate and WCFF in the FB1 and FB5 models, respectively.

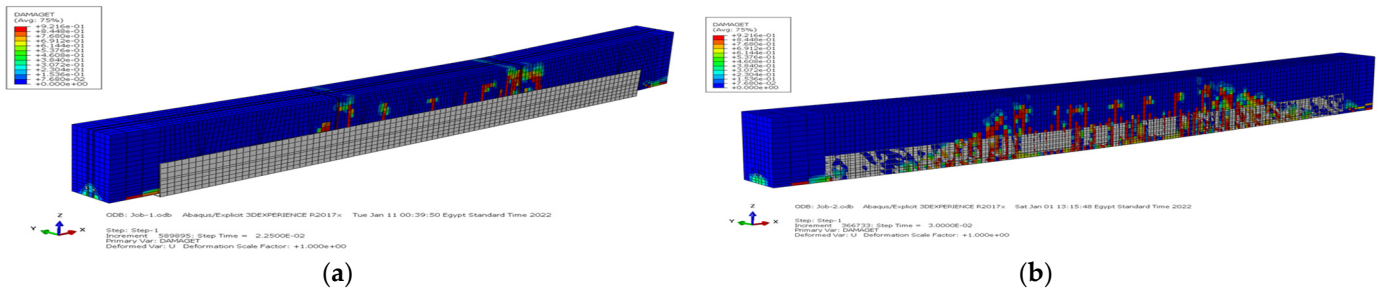


Figure 19. Damage of FE model: (a) FB1; (b) FB5.

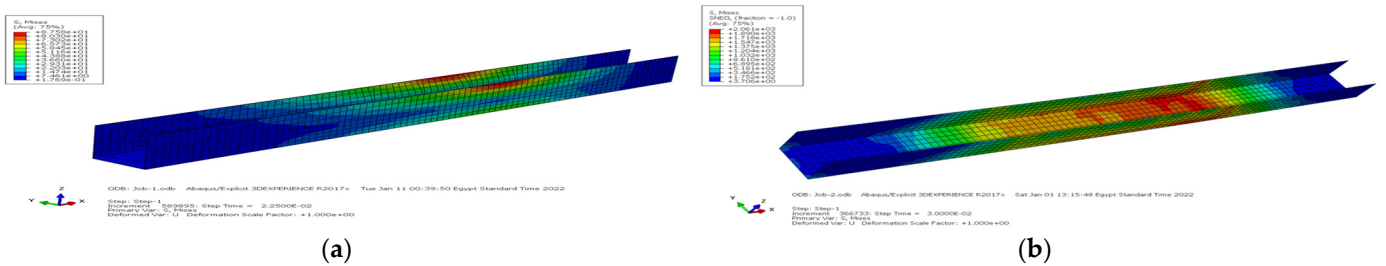


Figure 20. The stress distribution: (a) steel plate stress for FB1; (b) WCFF stress for FB5.

7.4.3. Addition of Steel Plate and WCFF to the Tension Side (FB3, FB7)

In the flexural damage tests, the beams equipped with a steel plate and woven carbon fiber fabric (WCFF) experienced ultimate loads of 318.22 kN and 312.22 kN, respectively. The initiation of the first crack occurred at loads of 95.46 kN and 79.61 kN for the steel plate and WCFF models, respectively. Figure 21 visually depicts the crack patterns observed in FB3 and FB7 after testing. These figures provide insights into the failure modes and crack propagation within the beams. For a more detailed understanding of stress distribution, Figure 22 showcases the stress distribution of the steel plate and WCFF in the FB3 and FB7 models, respectively.

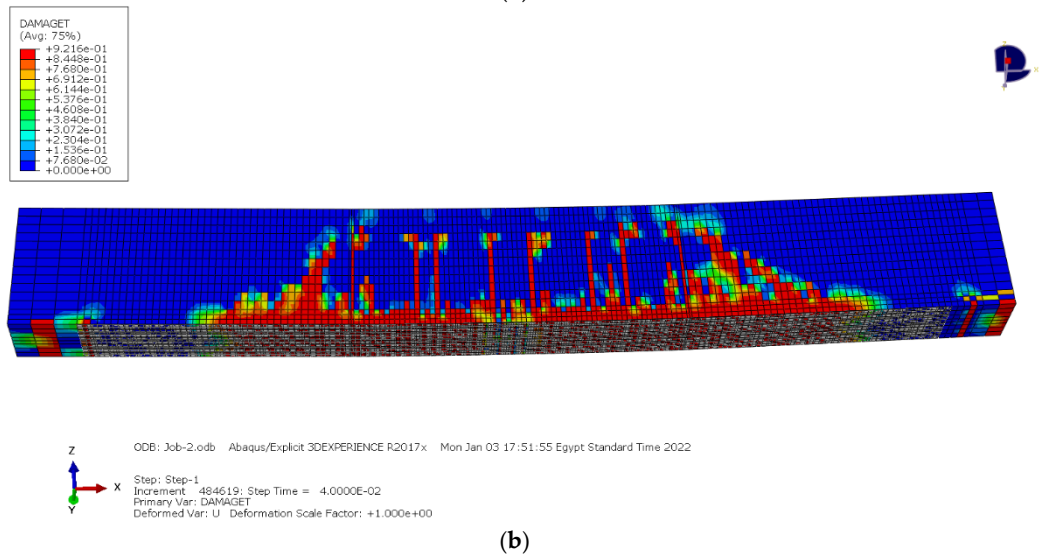
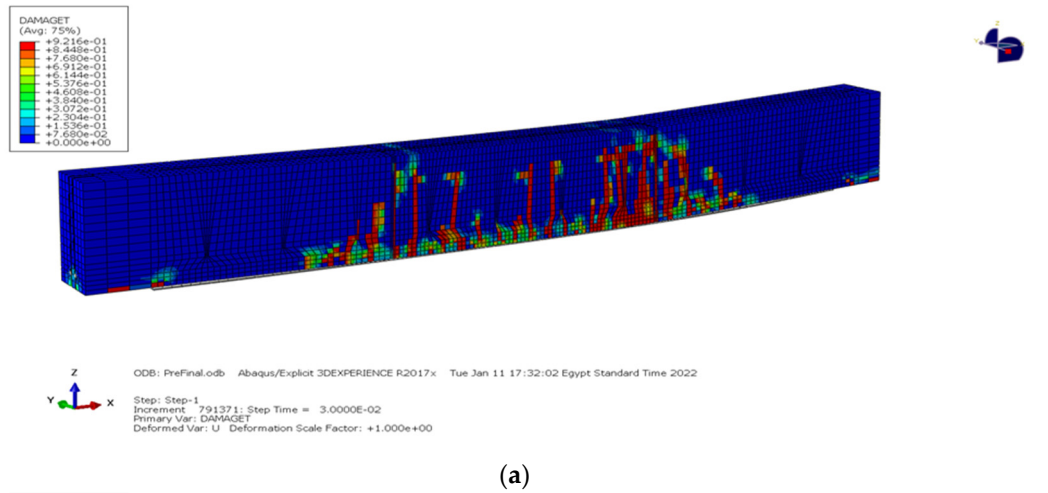


Figure 21. Damage of FE model: (a) FB3; (b) FB7.

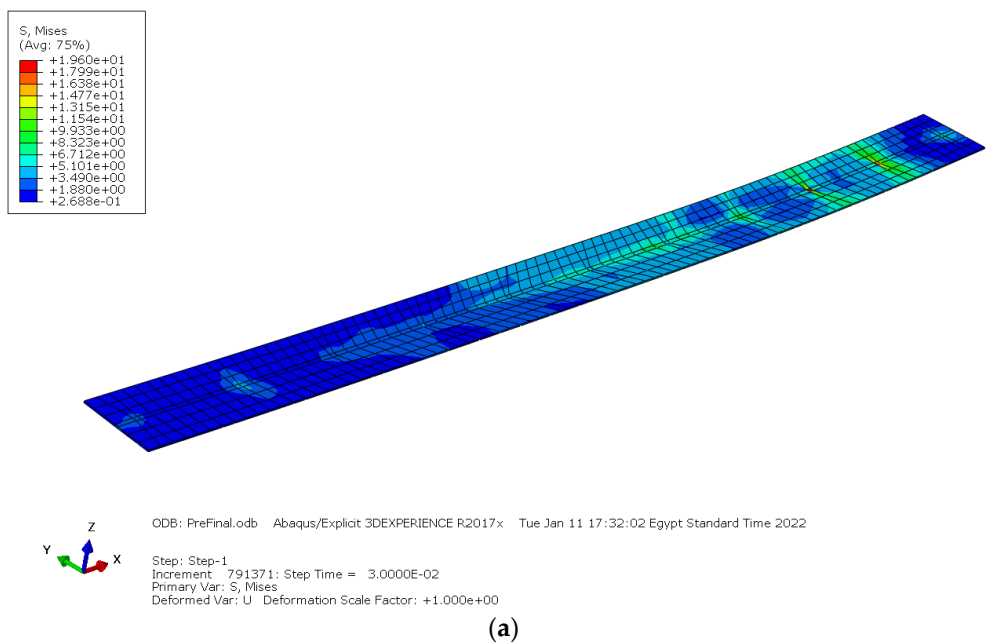


Figure 22. Cont.

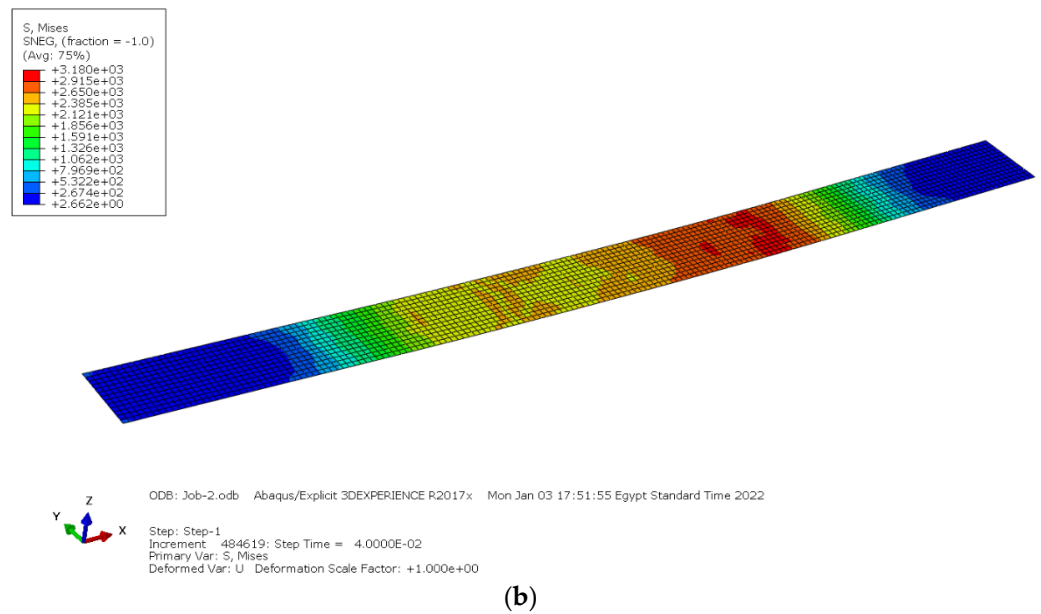


Figure 22. The stress distribution: (a) steel plate stress for FB3; (b) WCCF stress for FB7.

7.5. Finite Element Model Results for the Shear Test Series

7.5.1. Control Beam (CS)

In the shear damage test, the control beam with cables experienced ultimate failure at a load of 270.23 kN. The initiation of the first crack occurred at a load of 122.95 kN. Figure 23 visually represents the crack pattern observed in the control beam with cables (CS) after testing, providing insights into the nature and extent of cracking within the beam. For a further analysis of the structural response, Figure 24 presents the maximum deflection of the control beam. The maximum deflection for the sample reached 8.48 mm, and the average deflection at mid-span was 3.87 mm. These measurements contribute to characterizing the deformation and overall performance of the control beam under the applied shear loading conditions.

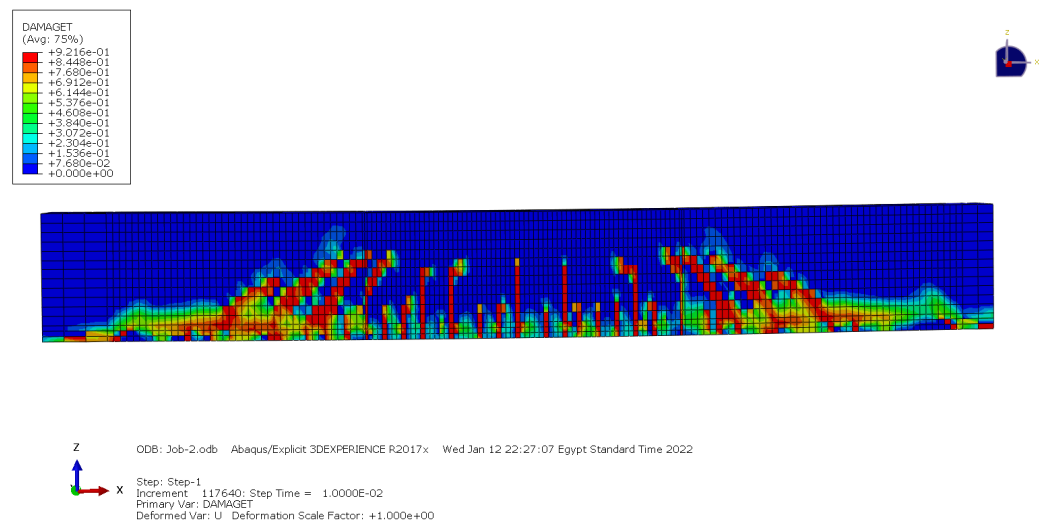


Figure 23. Damage of FE model for control beam CS.

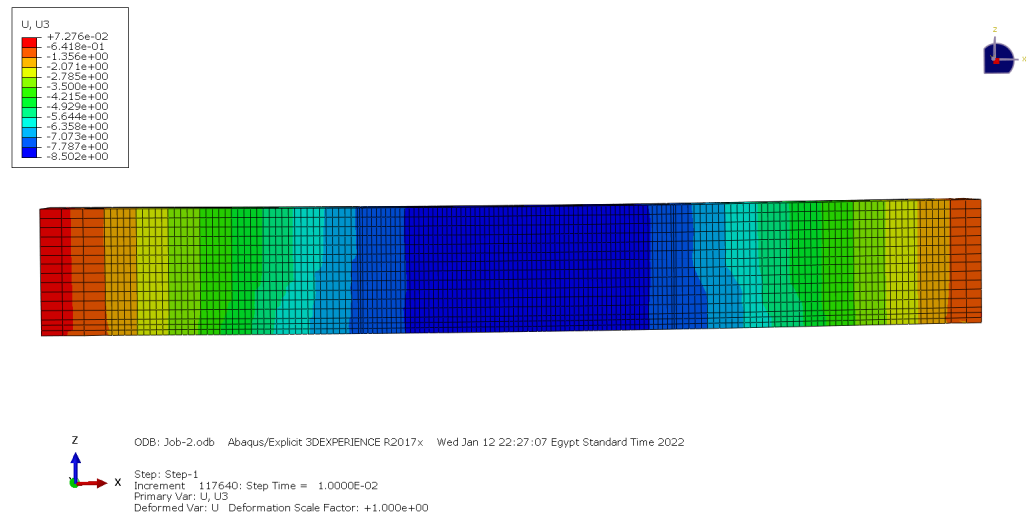
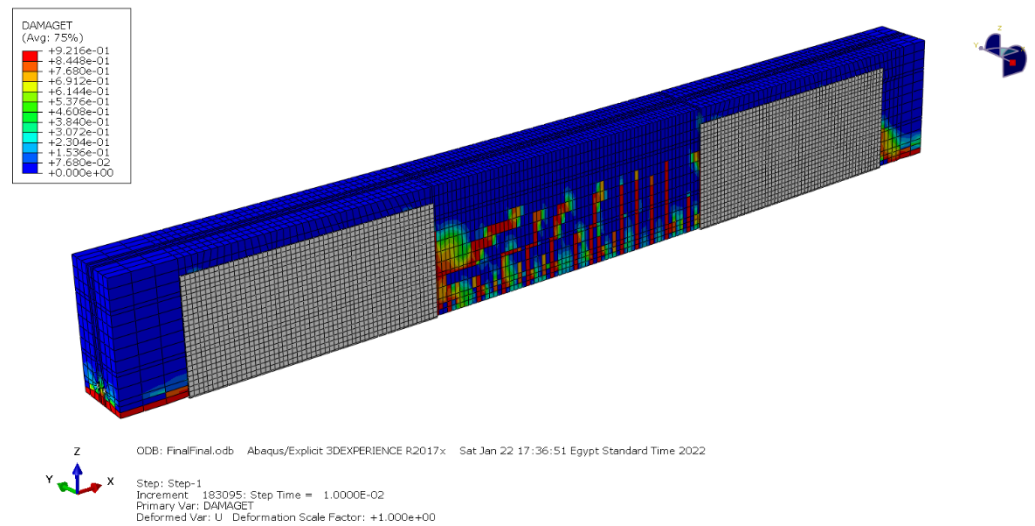


Figure 24. The max deflection of FE model for control beam CS.

7.5.2. Addition of Steel Plate and WCFF U-Shaped (SB1, SB5)

In the shear damage tests, the beams equipped with a U-shaped steel plate and woven carbon fiber fabric (WCFF) experienced ultimate loads of 460.88 kN and 460.88 kN, respectively. The initiation of the first crack occurred at loads of 193.57 kN and 161.31 kN for the U-shaped steel plate and WCFF models, respectively. Figure 25 visually depicts the crack patterns observed in SB1 and SB5 after testing, providing insights into the failure modes and crack propagation within the beams. For a more detailed understanding of stress distribution, Figure 26 showcases the stress distribution of the steel plate and WCFF in the SB1 and SB5 models, respectively.



(a)

Figure 25. Cont.

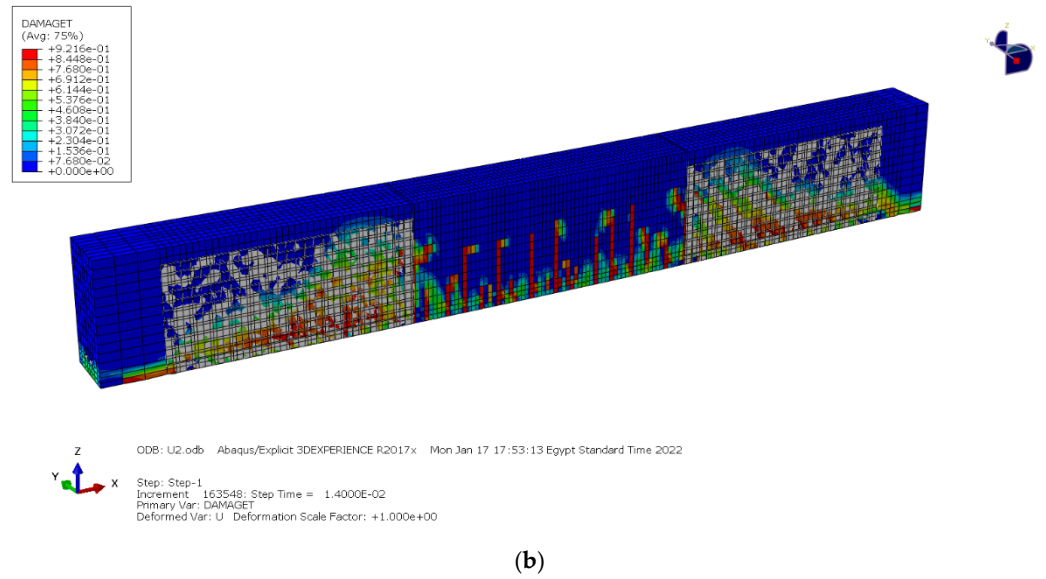


Figure 25. Damage of FE model: (a) SB1; (b) SB5.

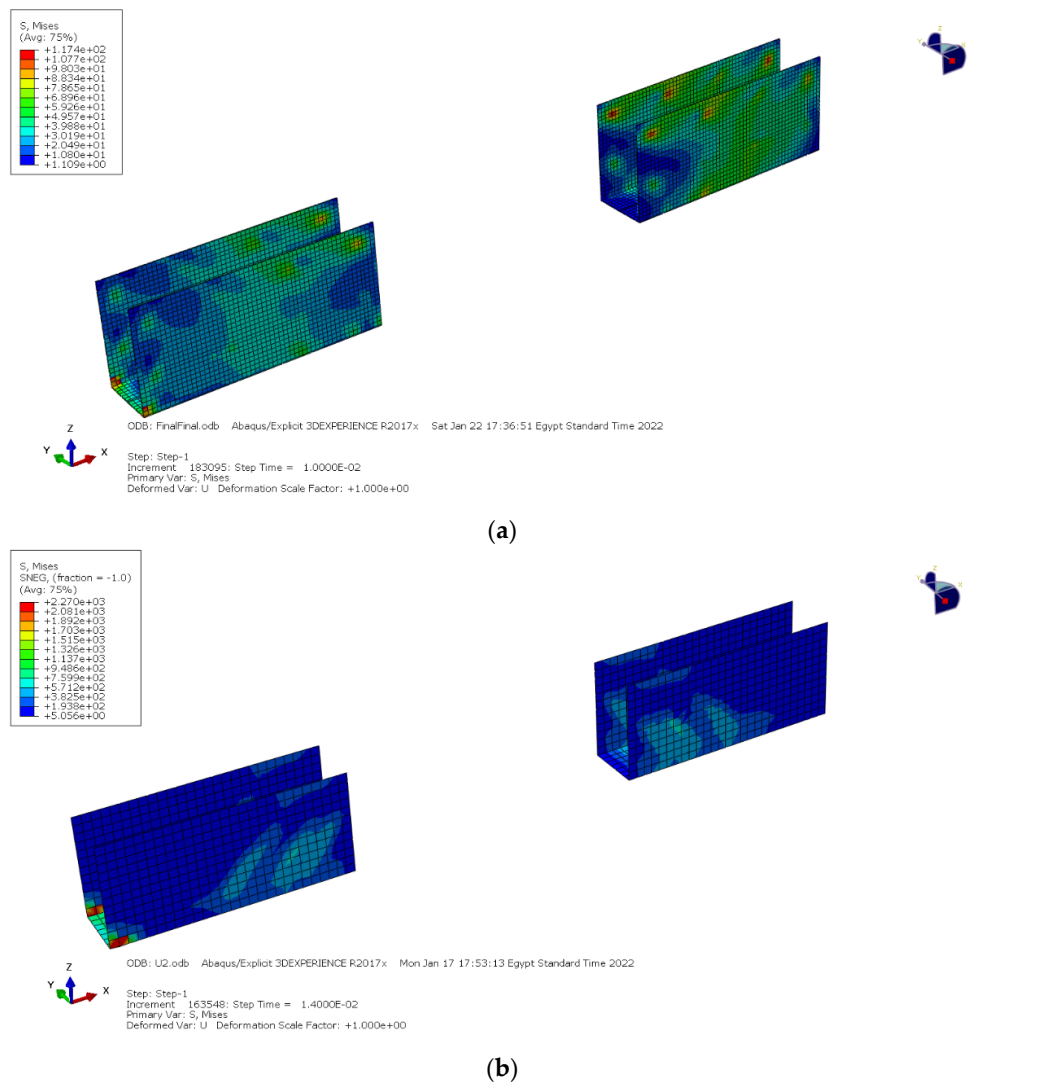


Figure 26. The stress distribution: (a) steel plate stress for SB1; (b) WCFB stress for SB5.

7.5.3. Addition of Steel Plate and WCFF Straps (SB3, SB7)

In the shear damage tests, the beams equipped with steel plates and woven carbon fiber fabric (WCFF) straps experienced ultimate loads of 281.55 kN and 397.37 kN, respectively. The initiation of the first crack occurred at loads of 126.70 kN and 143.05 kN for the steel plate and WCFF straps models, respectively. Figure 27 visually depicts the crack patterns observed in SB3 and SB7 after testing, providing insights into the failure modes and crack propagation within the beams. For a more detailed understanding of stress distribution, Figure 28 showcases the stress distribution of the steel plate and WCFF in the SB3 and SB7 models, respectively.

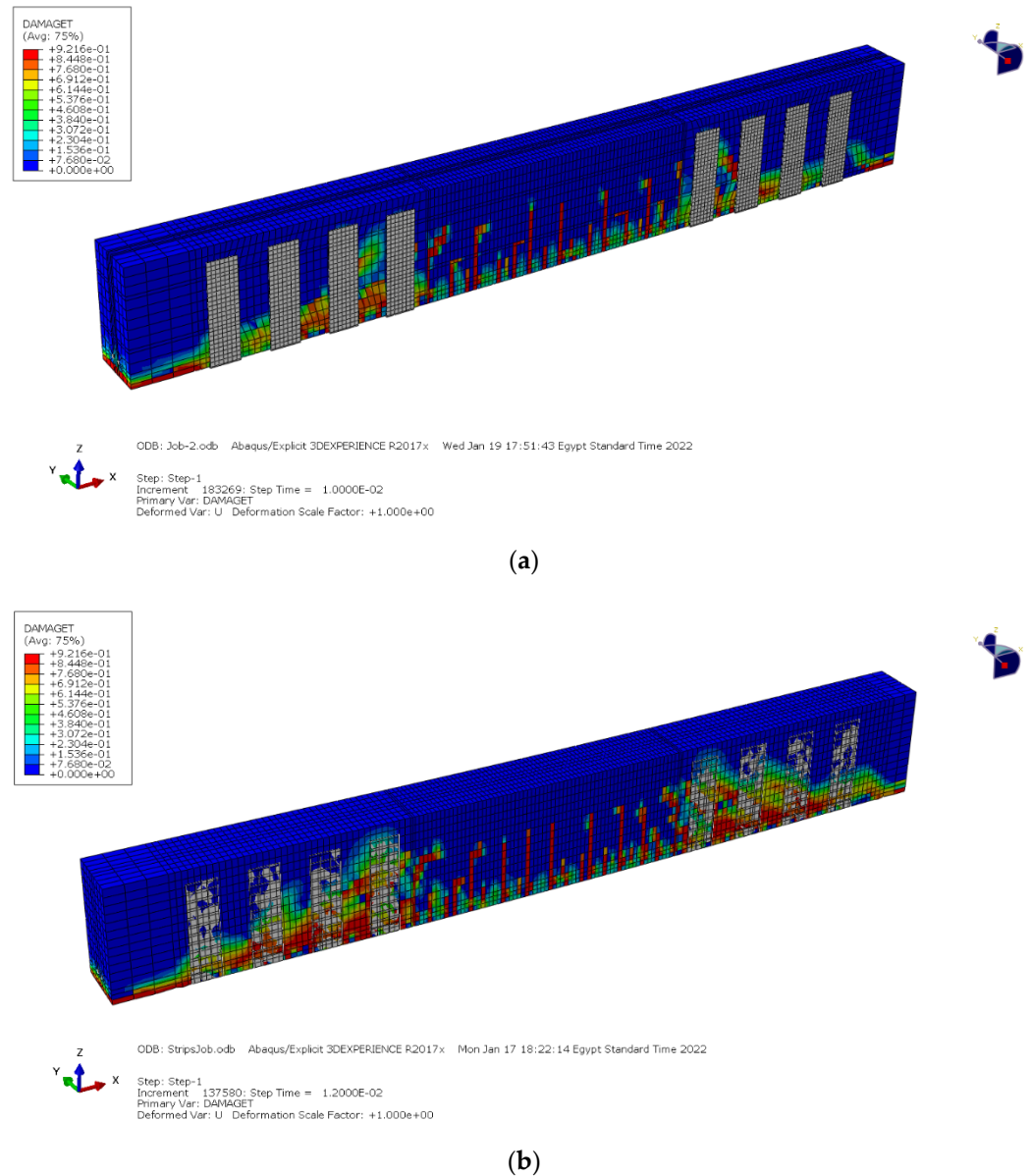


Figure 27. Damage of FE model: (a) SB3; (b) SB7.

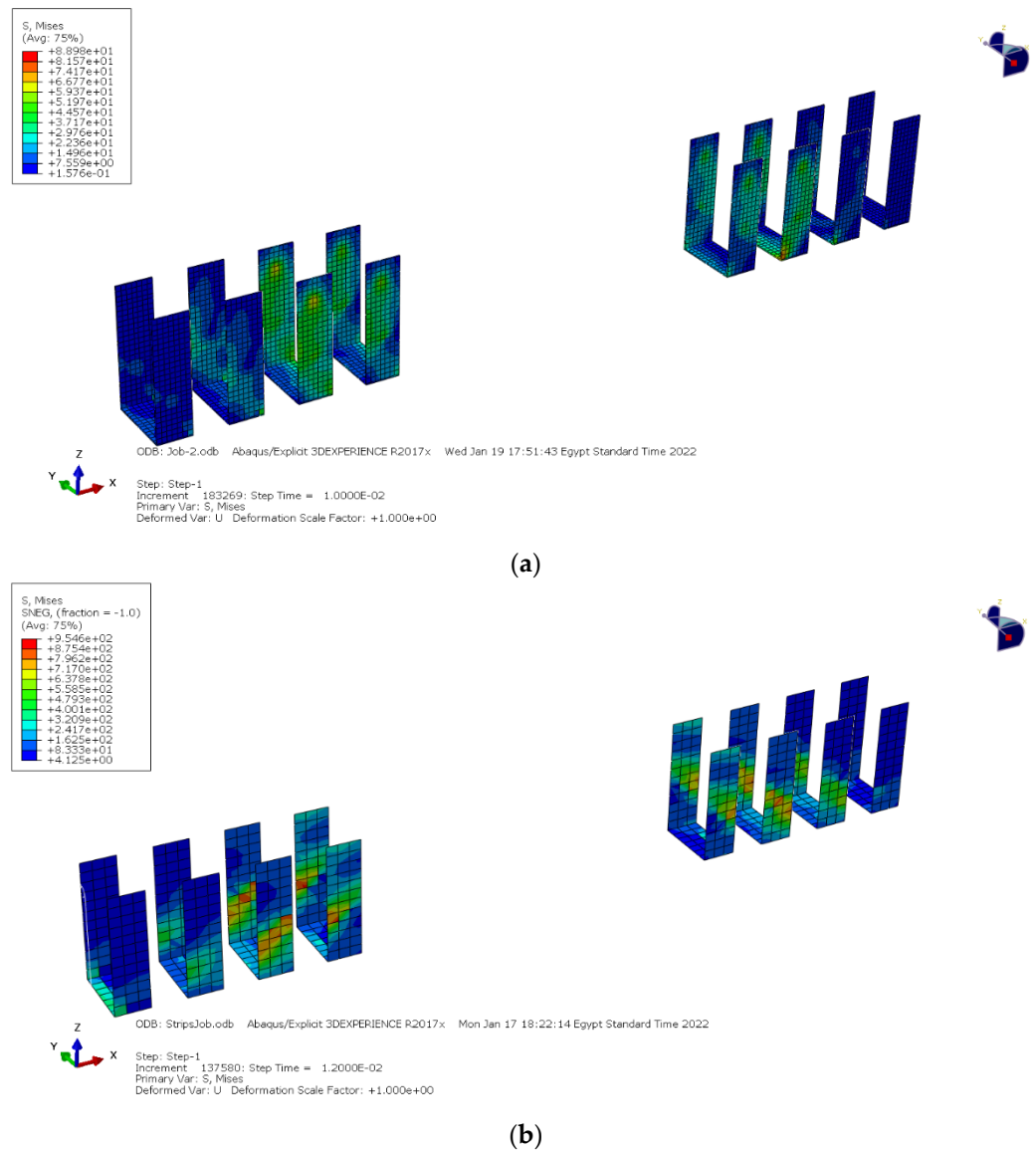


Figure 28. The stress distribution: (a) steel plate stress for SB3; (b) WCCF stress for SB7.

8. Comparison between FEM and Experimental Test Results

8.1. Ultimate Loads

Figure 29 provides a comparison of the ultimate failure loads between the experimental and finite element modeling (FEM) results for both flexure- and shear-tested beams. The differences in the ultimate loads between the experimental and FEM results are reported for various beam configurations. For the control beam in the flexure test series (CF) and the control beam in the shear test series (CS), the differences in the ultimate loads were approximately 3% and 5%, respectively. For the beams strengthened, with respect to their flexural properties, using steel plates and WCCF wrapping (FB1, FB3, FB5, and FB7) the differences in the ultimate loads between the experimental and FEM results were around 3%, 5%, 2%, and 1%, respectively. For the beams strengthened, with respect to their shear properties, using steel plates and WCCF wrapping (SB1, SB3, SB5, and SB7) the differences in the ultimate loads between the experimental and FEM results were approximately 17%, 14%, 1%, and 6%, respectively. These differences in the ultimate loads between the experimental and FEM results provide insights into the accuracy and reliability of the finite element model in predicting the structural behavior of the tested beams under both flexure and shear conditions.

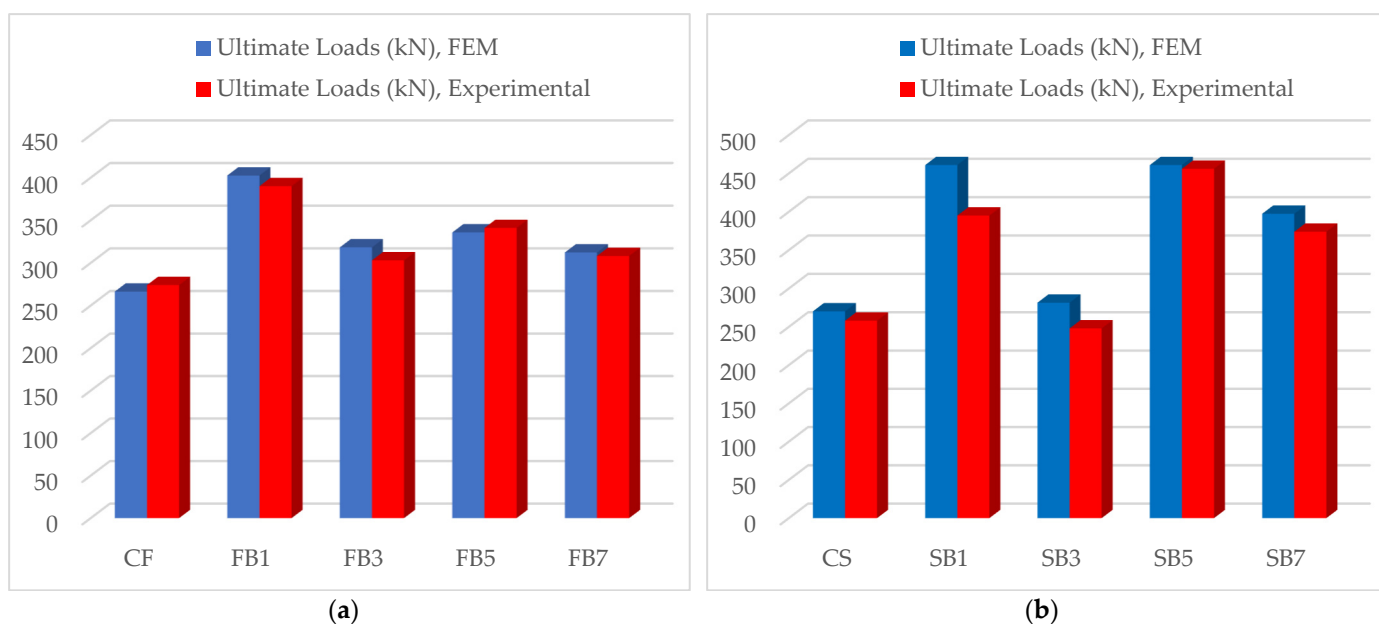


Figure 29. Comparison between experimental and FEM results of ultimate loads for (a) flexure-tested beams and (b) shear-tested beams.

8.2. Max Deflection

Figure 30 illustrates a comparison of the maximum deflection between the experimental and finite element modeling (FEM) results for both the flexure- and shear-tested beams. The differences in the maximum deflection between the experimental and FEM results are reported for various beam configurations. For the control beam in the flexure test series (CF) and the control beam in the shear test series (CS), the differences in the maximum deflection were approximately 2% and 2%, respectively. For the beams strengthened, with respect to their flexure properties, using steel plates and WCCF wrapping (FB1, FB3, FB5, and FB7) the differences in the maximum deflection between the experimental and FEM results were around 12%, 1%, 4%, and 5%, respectively. For the beams strengthened, with respect to their shear properties, using steel plates and WCCF wrapping (SB1, SB3, SB5, and SB7) the differences in the maximum deflection between the experimental and FEM results were approximately 8%, 8%, 0.3%, and 10%, respectively. These differences in the maximum deflection between the experimental and FEM results provide insights into the accuracy and reliability of the finite element model in predicting the deformation characteristics of the tested beams under both flexure and shear conditions.

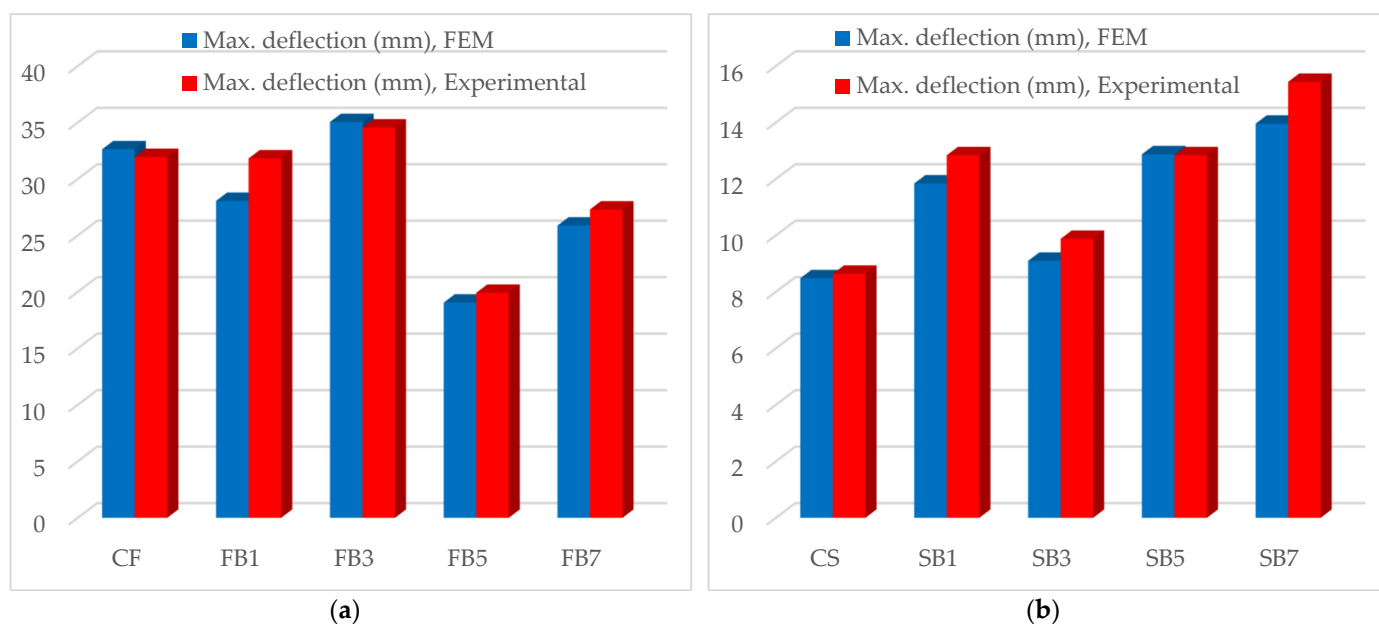


Figure 30. Comparison between experimental and FEM results of max deflection for (a) flexure-tested beams and (b) shear-tested beams.

9. Conclusions

From the experimental and numerical studies that were carried out on prestressed reinforced concrete beams strengthened with external steel plates and woven carbon fiber fabric, the following conclusions can be drawn:

- In summary, all strengthening techniques led to notable improvements in both flexural and shear strength outcomes when compared to the respective control beams. Specifically, the use of U-shaped steel plates resulted in significant increases between 57% and 97% in the first crack loads and between 14% and 48% in the ultimate loads for the prestressed concrete beams, strengthened with respect to their flexural properties. Likewise, woven carbon fiber fabric (WCFF) wrapping demonstrated increases between 27% and 35% in the first crack loads and between 17% and 29% in the ultimate loads.
- In terms of deflection, U-shaped steel plates and WCFF wrapping contributed to increases ranging from 25% to 29% and 27% to 38%, respectively, compared to the control beams.
- For prestressed concrete beams, strengthened with respect to their shear properties, the application of U-shaped steel plates yielded increases between 2% and 63% in the first crack loads and between 11% and 60% in the ultimate loads. WCFF wrapping, in turn, showed increases between 19% and 32% in the first crack loads and between 45% and 79% in the ultimate loads.
- Furthermore, the finite element model's results demonstrated congruence with the experimental outcomes, affirming the efficacy of the presented model. Notably, the maximum difference in the ultimate load for the prestressed concrete beams, strengthened with respect to their flexural properties, was approximately 5%, and the mid-span deflection showed a variance of about 9%.

Based on the conclusions of the current study the following recommendations are made for future research in woven carbon fiber fabric (WCFF) flexural and shear strengthening:

- Strengthening of pre-tension concrete beams could be carried out using more layers and angles of woven carbon fiber fabric (WCFF) wrapping.
- Strengthening of pre-tension concrete beams could be achieved using externally bonded hybrid fiber-reinforced polymer (HyFRP) laminates.

Author Contributions: Validation, A.S.E., P.S., K.K. and M.M.; formal analysis, M.G.A. and K.K.; investigation, A.S.E., K.K., M.M., P.S. and M.G.A.; resources, A.S.E. and M.G.A.; data curation, A.S.E. and M.G.A.; writing—original draft preparation, M.G.A., A.S.E., K.K. and M.M.; writing—review and editing, P.S., K.K., M.M. and M.G.A.; visualization, M.G.A. and K.K.; supervision, M.G.A. and K.K.; project administration, K.K., M.M. and M.G.A.; funding acquisition, M.M., P.S. and K.K. All authors have read and agreed to the published version of the manuscript.

Funding: This work was supported by the Cultural and educational grant agency of the Ministry of Education of the Slovak Republic's KEGA project 009TUKE-4/2023.

Data Availability Statement: Data are contained within the article.

Acknowledgments: This work was supported by grant KEGA 009TUKE-4/2023 of the Slovak Grant Agency.

Conflicts of Interest: The authors declare no conflict of interest.

References

1. Ravichandran, A.; Kothandaraman, S.; Zealakshmi, D. Flexural Behavior of Confined Hybrid Fiber in the Plastic Hinging Region of the High Strength Concrete Beam. *Indian J. Sci. Technol.* **2016**, *9*, 1–5.
2. Ravichandran, A.; Kothandaraman, S.; Zealakshmi, D. Prediction of Flexural Performance of Confined Hybrid Fiber Reinforced High Strength Concrete Beam by Artificial Neural Networks. *Indian J. Sci. Technol.* **2016**, *9*, 1–6.
3. Sim, C.; Tadros, M.; Gee, D.; Asaad, M. Flexural design of precast, prestressed ultra-high-performance concrete members. *PCI J.* **2020**, *65*, 35–61. [[CrossRef](#)]
4. Lei, D.; Chen, G.; Chen, Y.; Ren, Q. Experimental research and numerical simulation of RC beams strengthened with bonded steel plates. *Sci. China Technol. Sci.* **2012**, *55*, 3270–3277.
5. Al-Hassani, H.; Al-Ta'an, S.; Mohammed, A. Behavior of Damaged Reinforced Concrete Beams Strengthened with Externally Bonded Steel Plate. *Tikrit J. Eng. Sci.* **2013**, *20*, 48–59. [[CrossRef](#)]
6. Daouadji, T.H. Analytical and numerical modeling of interfacial stresses in beams bonded with a thin plate. *Adv. Comput. Des.* **2017**, *2*, 57–69. [[CrossRef](#)]
7. Altin, S.; Anil, Ö.; Kora, M.E. Improving shear capacity of existing RC beams using external bonding of steel plates. *Eng. Struct.* **2005**, *27*, 781–791. [[CrossRef](#)]
8. Aykac, S.; Kalkan, I.; Uysal, A. Strengthening of reinforced concrete beams with epoxy-bonded perforated steel plates. *Struct. Eng. Mech.* **2012**, *44*, 735–751. [[CrossRef](#)]
9. Alam, M.A.; Sami, A.; Mustapha, K.N. Embedded Connectors to Eliminate Debonding of Steel Plate for Optimal Shear Strengthening of RC Beam. *Arab. J. Sci. Eng.* **2017**, *42*, 4053–4068. [[CrossRef](#)]
10. Esfahani, M.R.; Kianoush, M.R.; Tajari, A.R. Flexural behavior of reinforced concrete beams strengthened by CFRP sheets. *Eng. Struct.* **2007**, *29*, 2428–2444. [[CrossRef](#)]
11. Rasheed, H.; Abdalla, J.; Hawileh, R.; Al-Tamimi, A. Flexural behavior of reinforced concrete beams strengthened with externally bonded Aluminum Alloy plates. *Eng. Struct.* **2017**, *147*, 473–485. [[CrossRef](#)]
12. Abdalla, J.; Abu-Obeidah, A.; Hawileh, R.; Rasheed, H. Shear strengthening of reinforced concrete beams using externally-bonded aluminum alloy plates: An experimental study. *Constr. Build. Mater.* **2016**, *128*, 24–37. [[CrossRef](#)]
13. Rakgate, S.M.; Dundu, M.S.M. Strength and ductility of simple supported R/C beams retrofitted with steel plates of different width-to-thickness ratios. *Eng. Struct.* **2018**, *157*, 192–202. [[CrossRef](#)]
14. Askar, M.K.; Hassan, A.F.; Al-Kamaki, Y.S. Flexural and shear strengthening of reinforced concrete beams using FRP composites: A state of the art. *Case Stud. Constr. Mater.* **2022**, *17*, e01189. [[CrossRef](#)]
15. Derkowski, A.; Walczak, R. Possibilities of increasing effectiveness of rc structure strengthening with frp materials. *Materials* **2021**, *14*, 1387. [[CrossRef](#)] [[PubMed](#)]
16. Vijayan, D.S.; Revathy, J. Flexural Response of Fibre Reinforced Polymer Laminated Pre-stressed Concrete Beams. *Indian J. Sci. Technol.* **2016**, *9*, 1–6. [[CrossRef](#)]
17. Hussien, O.F.; Elafandy, T.E.; Abdelrahman, A.S.; Abdel-Bakry, S.A.; Nasr, E.A. Behavior of bonded and unbonded prestressed normal and high strength concrete beams. *Hous. Build. Natl. Res. Cent. J.* **2012**, *8*, 239–251. [[CrossRef](#)]
18. Revathy, J.; Saranya, S.; Illakkiya, B. Behavior of Prestressed Concrete Beams Strengthened with Externally Bonded Fiber Reinforced Polymer Laminates. *Int. J. Struct. Anal. Des.* **2014**, *1*, 60–64.
19. Hurukadli, P.; Bharti, G.; Shukla, B.K. Behavior of fiber reinforced polymer laminates strengthening prestressed concrete beams. *Mater. Today Proc.* **2023**, *78*, 731–737. [[CrossRef](#)]

20. Siddika, A.; Al-Mamun, M.d.A.; Ferdous, W.; Alyousef, R. Performances, challenges and opportunities in strengthening reinforced concrete structures by using FRPs—A state-of-the-art review. *Eng. Fail. Anal.* **2020**, *111*, 104480. [[CrossRef](#)]
21. Dassault Systèmes. *Abaqus User's Guide*; Dassault Systèmes: Velizy-Villacoublay, France, 2013.

Disclaimer/Publisher's Note: The statements, opinions and data contained in all publications are solely those of the individual author(s) and contributor(s) and not of MDPI and/or the editor(s). MDPI and/or the editor(s) disclaim responsibility for any injury to people or property resulting from any ideas, methods, instructions or products referred to in the content.